Neutron Production from the Fracture of Piezoelectric Rocks

A. Widom and J. Swain
Physics Department, Northeastern University, Boston MA, USA

Y.N. Srivastava
Department of Physics & INFN, University of Perugia, Perugia, IT

A theoretical explanation is provided for the experimental evidence that fracturing piezoelectric rocks produces neutrons. The elastic energy micro-crack production ultimately yields the macroscopic fracture. The mechanical energy is converted by the piezoelectric effect into electric field energy. The electric field energy decays via radio frequency (microwave) electric field oscillations. The radio frequency electric fields accelerate the condensed matter electrons which then collide with protons producing neutrons and neutrinos.

PACS numbers: 62.20.mm,81.40.Np,03.75.Be,14.20.Dh

I. INTRODUCTION

There has been considerable evidence of high energy particle production during the fracture of certain kinds of crystals[1–6]. In particular, fracture induced nuclear transmutations and the production of neutrons have been clearly observed[7–14]. The production of neutrons appears greatly enhanced if the solids being fractured are piezoelectric[15] materials. Our purpose is to describe theoretically the manner in which the mechanical pressure in a piezoelectric stressed solid about to fracture can organize the energy so that neutrons can be produced.

The nuclear physics involves a standard weak interaction wherein collective radiation plus an electron can be captured by a proton to produce a neutron plus a neutrino

$$(\text{radiation energy}) + e^- + p^+ \to n + \nu_e. \qquad (1)$$

The required collective radiation energy may be produced by the mechanical elastic energy storage via the piezoelectric effect. By the *definition* of a *piezoelectric material*, the conversions of energy of the form

$$(\text{elastic energy}) \iff (\text{electric energy}) \qquad (2)$$

are allowed.

In terms of the electric field $\mathbf{E}$ and the crystal strain tensor w, the precise definition of the piezoelectric tensor β is discussed in Sec.II. The final result may be expressed as the effective interaction Hamiltonian

$$\mathcal{H}_{\rm int} = -\int \beta_{i,jk} E_i w_{jk} d^3\mathbf{r}, \qquad (3)$$

wherein the tensor coefficients $\beta_{i,jk}$ describe piezoelectricity as shown in FIG. 1. Some implications of the conversion from mechanical energy into electromagnetic energy are quite striking. For example, a piezoelectric ignition system can be constructed wherein a sharp mechanical impulse to a piezoelectric material can induce a sharp voltage spike across the sample with the resulting spark igniting a fire in a surrounding gas. More dramatically, the rocks crushed in earthquakes contain piezoelectric quartz. The mechanical impulse causing micro-cracks in the rocks can thereby produce impulse earthquake lightning flashes.

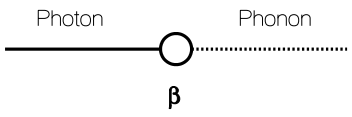

FIG. 1: Shown is the Feynman diagram exhibiting the change of a phonon described by the tensor strain w into a photon described by the vector electric field $\mathbf{E}$ and vice versa. The piezoelectric coupling strength tensor $\beta_{i,jk}$ is exhibited in the interaction Hamiltonian Eq.(3)

In Sec.III we review the stresses and strains which accompany micro-cracks in rocks that are being fractured. Elasticity theories of such micro-cracks are well known[16–18]. The central result is as follows. If $\sigma_{\rm bond}$ denotes the elastic stress required to break the chemical bonds on an area of a micro-crack and $\gamma_{\rm s}$ denotes the surface tension of the free face of a crack, then the fracture stress σ_F required to create a crack of half length a is given by

$$\sigma_F = \sqrt{\frac{\sigma_{\rm bond}\gamma_{\rm s}}{a}} \quad \Rightarrow \quad \sigma_F \ll \sigma_{\rm bond} \qquad (4)$$

for brittle fracture.

In Sec.IV, the manner in which the conversion of mechanical to electrical energy takes place is explored. It is shown that copious electromagnetic energy is emitted in the radio frequency microwave regime. The radiation accelerates the electrons allowing for nuclear transmutations in forms following from Eq.(1). In the concluding Sec.V, the number of neutrons produced by rock fractures will be estimated.

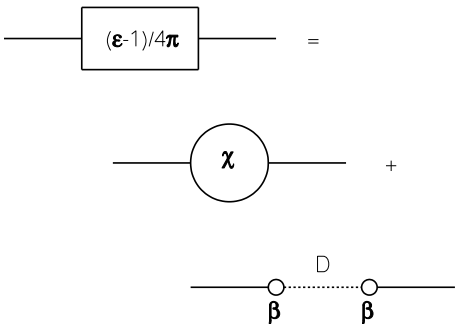

FIG. 2: The Feynman diagrams contributing to the polarization part of the photon propagator in a piezoelectric material are shown above. The resulting dielectric response in Eqs.(11) and (12), i.e. $\varepsilon_{ij}(\zeta)$, has a contribution due to mechanical phonon modes as exhibited above in diagrammatic form.

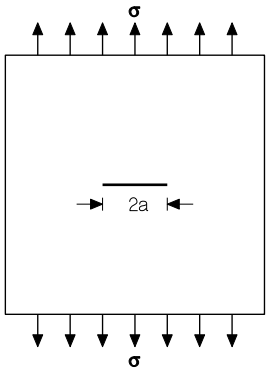

FIG. 3: A micro-crack is formed in solid under stress σ. The width of the micro-crack is $2a$ and the length (into the paper) of the crack is $L \gg a$. The half width a is the critical length size for forming the micro-crack as in Eq.(14).

II. PIEZOELECTRIC INTERACTIONS

The energy per unit volume U of a piezoelectric material obeys

$$dU = TdS + \sigma : d\mathsf{w} - \mathbf{P} \cdot d\mathbf{E}, \tag{5}$$

wherein T is the temperature, S is the entropy, σ is the stress tensor, w is the strain tensor, $\mathbf{P}$ is the electric dipole moment per unit volume and $\mathbf{E}$ is the electric field. The adiabatic piezoelectric tensor may be defined as

$$\beta_{i,jk} = \left(\frac{\partial P_i}{\partial w_{jk}}\right)_{S,\mathbf{E}} = -\left(\frac{\partial \sigma_{jk}}{\partial E_i}\right)_{S,\mathsf{w}}. \tag{6}$$

To quadratic order, the mechanical electric field interaction energy U_{int} follows from Eq.(6); It is

$$\beta_{i,jk} = -\frac{\partial^2 U(S,\mathsf{w},\mathbf{E})}{\partial E_i \partial w_{jk}} = -\frac{\partial^2 U(S,\mathsf{w},\mathbf{E})}{\partial w_{jk} \partial E_i}\ ,$$
$$U_{int} = -\beta_{i,jk} E_i w_{jk} + \dots\ , \tag{7}$$

leading to the quantum operator in the effective Hamiltonian and the Feynman diagram of Eq.(3).

The adiabatic electric susceptibility of the material at constant strain is defined

$$\chi_{ij} = \left(\frac{\partial P_i}{\partial E_j}\right)_{S,\mathsf{w}}, \tag{8}$$

while the same susceptibility at constant stress is given by

$$\tilde{\chi}_{ij} = \left(\frac{\partial P_i}{\partial E_j}\right)_{S,\sigma}, \tag{9}$$

The elastic response tensor,

$$D_{ijkl} = \left(\frac{\partial w_{ij}}{\partial \sigma_{kl}}\right)_{S,\mathbf{E}}, \tag{10}$$

determines the difference between between the two susceptibilities in Eq.(8) and (9); i.e. the thermodynamic identity is that

$$\tilde{\chi}_{ij} = \chi_{ij} + \beta_{i,lk} D_{lknm} \beta_{j.nm}. \tag{11}$$

For a complex frequency $\zeta = \omega + i\eta$ with $\eta = \Im m\ \zeta \geq 0$, there are dynamical electric susceptibilities $\tilde{\chi}_{ij}(\zeta)$ and $\chi_{ij}(\zeta)$. The dynamical version of Eq.(11) is easily obtained. Phonon modes described by the dynamical phonon propagator $D_{lknm}(\zeta)$ affect the dynamical susceptibilities via

$$\mathbf{D} = \mathbf{E} + 4\pi\mathbf{P},$$
$$\varepsilon_{ij}(\zeta) = \delta_{ij} + 4\pi\tilde{\chi}_{ij}(\zeta),$$
$$\tilde{\chi}_{ij}(\zeta) = \chi_{ij}(\zeta) + \beta_{i,lk} D_{lknm}(\zeta) \beta_{j.nm}. \tag{12}$$

Eq.(11) is the zero frequency limit $\zeta \to i0^+$ of Eq.(12). The dynamical dielectric response tensor $\varepsilon_{ij}(\zeta)$ appears in the polarization part of the photon propagator[19]. The Feynman diagrams contributing to the polarization part of the photon propagator in a piezoelectric system are shown in Fig. 2. These are equivalent to Eq.(12) and explain why mechanical acoustic frequencies appear in the electrical response of piezoelectric materials.

III. FRACTURE AND STRESS

Shown in FIG. 3 is a crystal under stress σ inducing a micro-crack of width $2a$ and length $L \gg a$. The energy U_b required to create a micro-crack of half width b and length L is given by[17]

$$u(b) = \frac{U_b}{L} = 4\gamma_s\ b - \pi \left[\frac{(1-\nu^2)\sigma^2}{\mathcal{E}}\right] b^2, \tag{13}$$

wherein γ_s is the surface tension of the micro-crack interface, $\mathcal{E}$ is the material Young's modulus and ν is the Poisson ratio.

A. Tensile Strength

The maximum of the elastic micro-crack energy per unit length ($\max_{b>0}\ u(b)$) represents the energy barrier to micro-crack creation. In detail,

$$u = \max_{b>0}\ u(b) \ \text{ at } \ b = a,$$
$$a = \frac{2\gamma_s}{\pi}\left[\frac{\mathcal{E}}{(1-\nu^2)\sigma_F^2}\right],$$
$$u = 2\gamma_s a = \frac{4\gamma_s^2}{\pi}\left[\frac{\mathcal{E}}{(1-\nu^2)\sigma_F^2}\right]. \tag{14}$$

The stress level σ_F which nucleates a micro-crack is thereby the well known result[20]

$$\sigma_F = \sqrt{\frac{2\gamma_s\mathcal{E}}{\pi(1-\nu^2)a}} \tag{15}$$

The tensile strength σ_F of the material is then given by Eq.(4) wherein the broken chemical bond strength

$$\sigma_{\rm bond} = \frac{2\mathcal{E}}{\pi(1-\nu^2)} \tag{16}$$

is determined by Young's modulus $\mathcal{E}$ and the Poisson ratio ν.

B. Numerical Estimates

Employing the values of material constants for fused quartz, we can estimate at least the powers of ten that would apply to piezoelectric rocks such as granite rocks. The values are

$$\gamma_s \sim 10^2\ \frac{\rm erg}{\rm cm^2}\ ,$$
$$\sigma_{\rm bond} \sim 10^{12}\ \frac{\rm erg}{\rm cm^3}\ ,$$
$$\sigma_F \sim 10^9\ \frac{\rm erg}{\rm cm^3}\ ,$$
$$a \sim 10^{-4}\ {\rm cm}\ , \tag{17}$$

in satisfactory agreement with the elastic theory as reviewed in Sec.III A.

Some comments are in order: (i) For quartz, the value of $a \sim 1$ micron. (ii) For the brittle fracture of quartz, the macroscopic fracture surface experimentally exhibits micro-cracks with a length $L \sim 20$ micron $\gg a$. (iii) As is usual in fractures $\sigma_F \ll \sigma_{\rm bond}$, i.e. $\sigma_F \sim 10^{-3}\sigma_{\rm bond}$ for the problem at hand. (iv) The velocity of sound v_s compared with the velocity of light c obeys $(v_s/c) \sim 10^{-5}$. The ratio of phonon frequencies to photon frequencies in cavities of similar length scales thereby obey

$$\left(\frac{\omega_{\rm phonon}}{\omega_{\rm photon}}\right) \sim 10^{-5} \quad \text{for similar sized cavities.} \tag{18}$$

The importance of the above Eq.(18) is that the phonon modes enter into the dynamic dielectric response function $\varepsilon(\omega + i0^+)$ in virtue of Eq.(12).

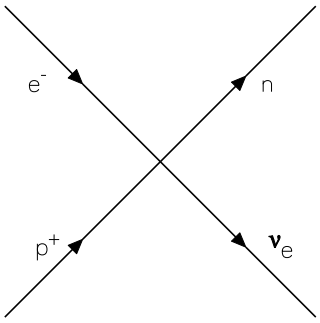

FIG. 4: Neutron production takes place via the standard Fermi weak interaction as shown above. The electron energy is renormalized $mc^2 \to W$ by condensed matter microwave radiation present as the stress approaches the fracture value σ_F. The coupling strength at the four Fermion vertex is G_F.

IV. NEUTRON PRODUCTION

The neutron production rate at the fracture stress σ_F is here considered due to energetic electrons scattering off protons which are naturally present in (say) granite as water or organic molecules. The Feynman diagram in the Fermi theory limit of the standard model is shown in FIG. 4 described in Eq.(1).

A. Electron Renormalized Energy W

To begin to analyze the production of neutrons via the reaction Eq.(1), one must calculate the mean energy of electrons in condensed matter when accelerated by an electric field

$$\frac{d\mathbf{p}}{dt} = e\mathbf{E}. \tag{19}$$

The electron energy is estimated to be

$$W = \sqrt{m^2c^4 + c^2\overline{|\mathbf{p}|^2}}. \tag{20}$$

If $P_{\mathbf{E}}(\omega)d\omega$ represents the the mean squared electric field strength in a bandwidth $d\omega$, then Eq.(19), implies

$$E^2 = \int_0^\infty P_{\mathbf{E}}(\omega)d\omega,$$
$$\overline{|\mathbf{p}|^2} = e^2\int_0^\infty P_{\mathbf{E}}(\omega)\frac{d\omega}{\omega^2}. \tag{21}$$

If Ω denotes the dominant frequency in the spectrum of electric field fluctuations, then Eq.(21) is more simply written

$$\overline{|\mathbf{p}|^2} = \frac{e^2E^2}{\Omega^2} \tag{22}$$

so that the ratio of the energy to the rest energy of the electron is

$$\beta = \frac{W}{mc^2} = \sqrt{1 + \left(\frac{eE}{mc\Omega}\right)^2} \ . \tag{23}$$

The value of $\beta > 1$ is critical for measuring whether or not there is sufficient radiation energy to allow for the reaction in Eq.(1).

B. Further Numerical Estimates at Fracture

To estimate the electric field, one notes that the stress at fracture σ_F is in large part due to the electric field strength

$$\sigma_F \sim \frac{E^2}{4\pi} \quad \Rightarrow \quad E \sim 10^5 \text{ Gauss}, \tag{24}$$

in virtue of Eq.(17). Since

$$\frac{e}{mc} \approx 1.75882915 \times 10^7 \ \frac{1}{\text{Gauss second}} \ , \tag{25}$$

one finds

$$\frac{eE}{mc} \sim \frac{10^{12}}{\text{second}} \ . \tag{26}$$

The frequency of a sound mode localized on a micro-crack of width $2a$ for a reasonable sound velocity in rock is in the microwave range

$$\Omega \sim \frac{10^9}{\text{second}} \tag{27}$$

One should then observe electromagnetic microwave emission when the sound mode is turned into an electromagnetic mode via the piezoelectric effect.

In virtue of Eqs.(23), (26) and (27) one finds $\beta \sim 30$. The threshold value of β for Eq.(1) to be possible without radiation is $\beta_0 \approx 2.53$ so that the energy renormalized by radiation is above threshold by a wide margin, i.e. $\beta \gg \beta_0$. The electron energies on the surface of a micro-crack in a stressed environment with an external stress σ_F obey

$$W \sim 15 \text{ MeV} \ . \tag{28}$$

The transition rate per unit time for Eq.(1) by the usual standard has been computed[21, 22] as

$$\Gamma(e^- + p^+ \to n + \nu_e) \approx \left(\frac{G_F m^2}{\hbar c}\right)^2 \left(\frac{mc^2}{\hbar}\right) \beta^2,$$

$$\Gamma(e^- + p^+ \to n + \nu_e) \approx 7 \times 10^{-3} \beta^2 \text{ Hz},$$
$$\Gamma(e^- + p^+ \to n + \nu_e) \sim 0.6 \text{ Hz} \quad \text{for} \quad \beta \sim 30. \tag{29}$$

The transition rate per unit time per unit area of micro-crack surfaces may be found from

$$\varpi_2 = n_2 \Gamma(e^- + p^+ \to n + \nu_e) \tag{30}$$

wherein n_2 is the number of protons per unit micro-crack area in the first few layers of the quartz granite. Typical values are

$$n_2 \sim 2 \times 10^{14} \ \frac{1}{\text{cm}^2} \quad \Rightarrow \quad \varpi_2 \sim 10^{15} \frac{\text{Hz}}{\text{cm}^2} \ . \tag{31}$$

If the fracture takes place with hydraulic fracture processes, then the neutron production rate will be about a factor of ten higher due to the higher water concentration on the micro-crack surface areas.

V. CONCLUSIONS

It is in the nature of piezoelectric matter that strong mechanical disturbances give rise to strong electromagnetic responses. This is true for piezoelectric rocks such as granite which contain large amounts of quartz. For large scale piezoelectric rock fracturing, as takes place in earthquakes, electromagnetic responses in many frequencies, from radio frequaecy to gamma ray frequancy, are to be expected. Some have attributed earthquake lights and/or lightning[23] to the phenomena discussed in this work.

We have employed the standard model of weak interactions along with the known theory of piezoelectric materials to explain the experimental evidence that fracturing piezoelectric rocks produces neutrons. We have also explained why such fracturing processes produce microwave radiation. The elastic energy micro-crack production ultimately yields the macroscopic fracture whose acoustic vibrations are converted into electromagnetic oscillations. The electromagnetic microwaves accelerate the condensed matter electrons which then scatter from protons to produce neutrons and neutrinos. This work also may have implications for a better understanding of radiative processes associated with earthquakes[24, 25].

[1] V.V. Karassey, N.A. Krotova and B.W. Deryagin, *Dokl. Akad. Nauk SSSR* **88**, 777 (1953).

[2] V.A. Klyuev, A.G. Lipson, Yu.P. Toporov, B.V. Deryagin, V.J. Lushchikov, A.V. Streikov, E.P. Shabalin, *Sov.*

Tech. Phys. Lett. **12**, 551 (1986).
[3] V. Klyuev et al., *Kolloidn. Zh.* **88**, 1001 (1987).
[4] G. Preparata, *Il Nuovo Cimento* **104**, 1259 (1991)
[5] K. Nakayama, N. Suzuki and H. Hashimoto, *Journal of Physics* **D 25**, 303 (1992)
[6] B. Lawn, "*Fracture of Brittle Solids*', Sec. 4.5, page 103, Cambridge University Press, Cambridge (1993)
[7] B.V. Derjaguin, A.G. Lipson, V.A. Kluev, D.M. Sakov and Yu.P. Toporov, *Nature*, **341** , 492 (1989)
[8] A. G. Lipson, D. M. Sakov, V. A. Klyuev and B. V. Deryagin, *JETP. Lett.* **49**, 675 (1989).
[9] B.V. Derjaguin, V.A. Kluev, A.G. Lipson, and Yu.P Toporov, *Physica* **B 167**, 189 (1990).
[10] T. Kaushik et al, *Phys. Lett.* **A 232**, 384 (1997).
[11] Y. Shioe et al., *Il Nuovo Cimento* **112** 1059 (1999).
[12] F. Cardone, A. Carpinteri, and G. Lacidogna, *Phys. Lett.* **A 373**, 862 (2009).
[13] A. Carpinteri and G. Lachidogna, *Strain* **45**, 332 (2009)
[14] M. Fuji et al., *Jpn. J, Appl. Phys*, **41**, 2115 (2002)
[15] L.D. Landau and E.M. Lifshitz, *Electrodynamics of Continuous Media*, Sec. 17, Pergamon Press, Oxford (1984).
[16] L.B. Fruend, *Dynamic Fracture Mechanics*, Cambridge University Press, Cambridge (1998).
[17] L.D. Landau and E.M. Lifshitz, *Theory of Elasticity*, Sec. 31, Pergamon Press, Oxford (1970).
[18] A.A. Griffith, *Proc. Roy. Soc.* **221**, 161 (1921).
[19] A.A. Abrikosov, Gorkov and I.E. Dzyaloshinskii, *Qunatum Field Theory Methods in Statistical Physics*, Chapter 6, Prentice Hall, Englewood Cliffs (1963).
[20] L.D. Landau and E.M. Lifshitz, *op. cit.* [17], page 146, Eq.(31.10).
[21] A.Widom and L. Larsen *Eur. Phys. J.* **C 46**, 107 (2006).
[22] Y.N. Srivastava, A. Widom and L. Larsen, *Pramana* **75** 617 (2010).
[23] M. Ikeya and S. Takaki, *Jpn. J. Appl. Phys.* **35**, L355 (1996).
[24] F.T. Freund, "*Rocks that Crackle and Sparkle and Glow: Strange Pre-Earthquake Phenomena*", Journal of Scientific Exploration **17**, no. 1, p. 37-71 (2003).
[25] S. Takaki and M. Ikeya, "*A Dark Discharge Model of Earthquake Lightning*", Japanese Journal of Applied Physics **37** Issue 9A, 5016 (1998).